Light induced proton pumping with a semiconductor: vision for PhotoProton lateral separation and robust manipulation

Hanna Maltanava,[‡] Sergey K. Poznyak,[‡] Daria V. Andreeva,[ǁ] Marcela C. Quevedo,[#] Alexandre C. Bastos,[#] João Tedim,[#] Mário G. S. Ferreira[#] and Ekaterina V. Skorb[†,]*

[†] Department of Chemistry and Chemical Biology, Harvard University, 12 Oxford Street, Cambridge 02138, MA, United States

[‡] The Research Institute for Physical Chemical Problems, Belarusian State University, Minsk 220030, Belarus

[ǁ] Center for Soft and Living Matter, Institute of basic science Ulsan, National Institute of Science and Technology, Ulsan 44919, Republic of Korea

[#] CICECO, Department of Materials and Ceramic Engineering, University of Aveiro, Aveiro 3810-193, Portugal

KEYWORDS: photocatalysis, TiO_2, pH gradient, nanoscale machinery, photoacid, chemical network

SIGNIFICANCE: Understanding how protons are spatiotemporally pumped in the system has a broad application in a wide range of pH-responsive adaptive materials. We introduce a reliable, minimal reagent consuming, stable inorganic light promoted proton pump with spatial and temporal separation of oxidation and reduction of water. Localized illumination was applied to a TiO_2 surface in solution for reversible spatially controlled "inorganic photoproton" cycling. The proton flux is pumped during irradiation of the surface of TiO_2 and dynamically maintained at the irradiated surface area, in the absence of any membrane or predetermined material structure. Mechanisms for this have been elaborated in the paper.

ABSTRACT: Energy transfer reactions are the key for living open systems, biological chemical networking and development of life inspired nanoscale machineries. It is a challenge to find simple reliable synthetic chemical networks providing a localization of the time dependent flux of matter. In this paper we introduce a reliable, minimal reagent consuming, stable inorganic light promoted proton pump. Localized illumination was applied to a TiO_2 surface in solution for reversible spatially controlled "inorganic photoproton" isometric cycling, the lateral separation of water splitting reactions. The proton flux is pumped during irradiation of the surface of TiO_2 and dynamically maintained at the irradiated surface area in the absence of any membrane or predetermined material structure. Moreover we spatially predetermine a transient acidic pH on the TiO_2 surface in the irradiated area with feedback-driven generation of a base as deactivator. Importantly we describe, how to effectively monitor the spatial localization of the process by *in situ* scanning ion selective electrode technique (SIET) measurements for pH and scanning vibrating electrode technique (SVET) for local photoelectrochemical studies. This work shows

the great potential for time- and space-resolved water splitting reactions for following investigation of pH stimulated processes in open systems with their flexible localization on a surface.

Today increased interest is focused on dynamic, non-equilibrium material properties varying with time: a life inspired nanoscale machinery (1-4). It involves needs for effective energy conversion with the focus on oscillation reactions (5), chemical networking (6), autocatalytic (7) and autoamplification (8) reactions, mimicking living systems (9), using cell metabolic biomolecules (10) and ions, e.g. proton gradients (11). Biological systems solve such an energy-management by developing unique sensory and adaptive capabilities, transport mechanisms guided with ions, proton gradients and chemical networks (12). It is very attractive to use light energy (13) conversion for modulation of simple, reliable chemical networking, easy to control, based on existing knowledge on reliable light sensitive materials. We question if a semiconductor, e.g. TiO_2, surface has a potential as effective photoactive surface to design light controllable networks of chemical reactions with the lateral separation of the two reactions of water splitting. Robust lateral separation and understanding are the keys to derive the system further broad prospects. A simple possible network can be light assisted generation of protons from water molecules and neutralization of H_3O^+ with OH^- (**Figure 1a**).

Moreover, recently we have discussed prospects of complex pH-active material systems (14) and introduced light-pH coupled oscillations of polymer assembly (15), cells dynamic switching (16), and protein recognition (17) on TiO_2 modified with polyelectrolytes. A vision of manipulating with spatiotemporal processes on titania remains untouched, which motivates the

present work—robust lateral separation of the two reactions of water splitting with prospects of lateral separation of dynamic properties of pH sensitive assemblies. The hypothesis here is, that photoholes and photoelectrons may exhibit anisometric mobilities on surfaces. This may lead to a spatiotemporal separation of reduction and oxidation processes, via the control of the isometry of the carrier mobility. Mechanisms for this have to be elaborated.

In general semiconductor materials have been used for artificial photosynthetic system development (18) and are also known to enable efficient solar water splitting (19). Surprisingly a network of chemical reactions on semiconductor surfaces for open systems is not discussed much, simultaneously having different surface/interface engineering strategies, such as band structure engineering (20), co-catalyst engineering (21). Much is known how to improve heterogeneous semiconductors in terms of charge separation and transfer, enhanced optical absorption, optimized band gap position, lowered cost and toxicity, and improved stability (22). Thus when the background of formation of spatially separated reactions on TiO_2 surfaces is associated with chemical reaction networking synergy, it is easy to further up-scale and improve the sustainability of the system.

A successful example of an application of such a spatial separation of photoreactions might be a photocatalytic lithography based on a TiO_2 layer (23). The feasibility of the inversion of metal images obtained by the chemical deposition of metals onto nanostructured TiO_2 exposed to high radiation doses has been demonstrated (24), as well as the generation of both negative and positive metallic patterns by varying the dose was reported (25).

Here we focus, at the beginning, on macro-scale, cm dimension surfaces, to control localization of different pH zones on the surface *vs*. irradiation. Localization of chemical species may lead to

a life inspired proton pump machinery for localization of chemical networks on the surface of TiO_2 in an open system, providing further prospects for designing far-from-equilibrium,(26) dynamic (27), oscillation gel materials (28), stimuli-responsive drug delivery systems (29), metastable nanoparticle assemblies (30), reactors to proliferate acidic and basic molecules (7). Moreover, a thorough understanding of electron and hole transfer thermodynamics and kinetics will lead to elucidating the key efficiency-limiting step and designing highly efficient solar-to-fuel conversion systems (31). In this paper, we provide not only evidence of the possibility of spatial and temporal localization of proton pumping on semiconducting TiO_2 with light induced water splitting, but also some potential opportunities for designing an open system with localization of both H^+ and OH^-.

RESULTS AND DISCUSSION

Here we concentrate on the light promoted reaction of water protonation (**Figure 1a**). Under supra bandgap irradiation of the surface of many semiconductors, e.g. TiO_2, photohole and photoelectron are generated (**Figure 1b**). In the scope of photocatalytic reactions one can assume the possible formation of H^+ and OH^- due to oxidation (ox) and reduction (red) reactions involving photogenerated charge carriers on the semiconductor surface. Surprisingly, the dynamics of the simplest reactions of the formation of proton and hydroxyl radical has not been highlighted before. Thus, our key idea is to use water splitting on a semiconductor, not focusing on the products H_2 and O_2, as usual, but on reactions that provide the formation of H^+ and OH^-. We focus on the possibility of transforming the energy of electromagnetic irradiation into a pH gradient in time and space near the TiO_2 surface. A photocatalytically active nanostructured

titanium dioxide film is the light sensitive part of the model system. An anodized titania nanotubular layer (32) on titanium was used as highly photoactive (15) one, where the dissipation of protons can be prolonged due to the porosity of the semiconductor layer that facilitates the proton detection.

A series of consecutive photocatalytic reactions leads to the development of reactive species that contribute to a pH shift. There are no data to what extent the pH can be altered laterally on semiconductor surface, e.g. TiO_2. Can the pH be changed locally from, for example, 7 to 4 during irradiation of the TiO_2 surface? Which processes are preferable in the irradiation zone: acidification or alkalinization? Does localization of H^+ and OH^- correlate with localization of the irradiated area? How flexible is localization of the process?

The inorganic surface and its nanostructuring may be involved in the reaction through process location as well as surface morphology, porosity, as important to prolonged effects of release of chemicals. The water oxidation reaction on TiO_2 is initiated by a nucleophilic attack of a H_2O molecule on the photogenerated hole at the O site bridging two Ti atoms and as a result TiO·HO–Ti and later TiOOH and TiOOTi are formed.(33) During these oxygen photoevolution reactions protons are released. At the same time, the photogenerated electrons reduce the surface $Ti(^{4+})$ enabling adsorption of H_2O, and then O_2 attacks it immediately to form superperoxo TiOO.(34) As a result a hydroxide ion OH^- is released. Then TiOO is reduced to peroxo $Ti(O_2)$ which evolves to hydroperoxo TiOOH upon protonation. At the end, the surface is covered by hydroxyl groups. However, there are no data on the localization of processes on certain areas.

Using the scanning vibrating electrode technique (SVET) (**Figure 2**) we spatially resolve the *in situ* establishment of the ionic current density in solution induced by the photoelectrochemical

processes on the surface of TiO_2 under local (**Figure 2c**) low intensity (*ca*. 5mW/cm^2) LED UV (365 nm) irradiation. It is important to discuss the efficiency of charge separation as first light stimulated process on TiO_2. SVET here is a unique tool to monitor the processes *in situ* at certain locations, which is important to follow the development of photoreactions and the consecutive chemical network stability. The technique allows different modes to monitor the local ionic currents in solution associated with the photocurrent: single spot inside the irradiation point (**Figure 2d**), line scan (**Figure 2e**), and maps of surface activity vs. irradiation spot (**Figure 2g-i**) before (**Figure 2g**), during (**Figure 2h**) and after irradiation (**Figure 2i**). Current *vs* potential curves were also measured (**Figure 2f**).

After turn-on of illumination, the photocurrent first presents a rapid response with an initial spiking of the photocurrent, indicating a rapid filling and discharging of defect states (35), and then a plateau for relatively constant collection from the active region is reached. In the case of two electrodes (36), TiO_2 working electrode and counter electrode, the photocurrent is caused by the separation of photo-generated electron–hole pairs within the photo-electrode: holes move to the TiO_2 surface, where they are trapped or captured by reduced species in the electrolyte, while the electrons are transported to the back contact via TiO_2. Here, in our case, we have only one electrode, and photoelectrons are transported to adjacent non-irradiated zones.

A fast and uniform photocurrent response is clearly observed for switch-on and -off events on SVET. A dark current is quickly achieved after irradiation switching off. During the stationary mode the current density line scans and current density maps associated with the photocurrent can be measured to determine the degree of localization. A dash red line of the moving probe is indicated in **Figure 2c**, and the corresponding current density is shown in **Figure 2e**. The ionic

current can be monitored *vs*. location of the irradiated spot. The precise value in the centre under the stationary mode is 80 $\mu A/cm^2$.

After irradiation is switched off, the current relaxation in solution is shown in lines acquired every 3 min. Within 3 min after the irradiation is switched off the current density drops to 10 $\mu A/cm^2$. 6 min after the irradiation is switched off no photocurrent is detected.

Imaging and localization (**Figure 2h**) of the positions of hole- or electron-induced reactions across the surface relative to its irradiation spot are also measured with SVET. No currents are detected before and after irradiation (**Figures 2g and 2i**), but during irradiation ionic currents appear in solution in response to localized surface irradiation, positive in the irradiated points and slightly negative in the rest of the surface.

Figure 2f shows the photocurrent density versus applied bias curves under chopped illumination for the two electrode configuration (TiO_2 working electrode and Pt counter-electrode). In comparison with the dark current, the photocurrent increases significantly with the positive scanning of the applied potential, indicating a standard n-type behavior of TiO_2. The on/off cycle measurements show well-defined photoresponse after turning-on and turning-off illumination. Moreover, the value of the onset potential (**Figure 2f inset**) for reverse cycle is shifted to the positive direction, which can be explained by a change of the surface pH (this effect was studied in detail *in situ* with the scanning ion selective electrode technique (**Figure 3**)).

For pH modulation with light it is important to understand, how photoinitiated processes on TiO_2 result in the transformation of light into a pH change, including localization of the effect. We apply SIET for mapping of the activity and migration of H^+ ions over the TiO_2 surface. Maps of

the pH are collected for pristine TiO_2: before illumination (**Figure 3a**); during illumination (**Figure 3b**); after switching off irradiation, and during 40 min relaxation (**Figure 3c**).

It is seen from the presented proton distribution maps, that under irradiation, indeed, as suggested in Figure 1, the reaction of the generation of protons is observed. The protons are pumped from irradiated TiO_2 and have a gradient over the surface. It is important to note here, that an existing approach for static and localized pH gradients relies on pre-defined configurations of the microelectrodes (37). However, in our case the big advantage is, that we can operate in an open system without any membranes or patterning, just changing the localization of the irradiation spot to provide a proton pump at different places and varying the intensity of illumination. In order to change the gradient patterns, the re-design and re-fabrication of photo-masks, microelectrodes and sometimes chip structures themselves are required (36). This flexibility of pH gradients is promising for suggestion of life inspired nanoscale machineries.

The action of different photoelectrochemical reactions on the TiO_2 surface under UV illumination seems to be the only plausible explanation for the observed local acidification and is consistent with the mechanism proposed in **Figure 1**. It is seen from the SIET pH maps (**Figure 3a-c**), that the system effectively produces microscale pH gradients. Such an engineering of pH gradients, proton pumping on TiO_2, can be important for various chemical and biological networks. The simplest discussed here is the water protonation and following system deactivation with hydroxyl ions (**Figure 1**). Instead of immobilized pH gradients in gels, microscale pH gradients in open systems provide new avenues for on-chip reaction networks, identification and transfer of proteins and large molecules.

The focused single spot measurement (**Figure 3d**) and line scan (**Figure 3e**) inside and across the irradiation spot, visibly prove the effect of acidification in the irradiation spot and a slight increase of the pH in the remaining area. In comparison with SVET measurements after switching off irradiation, the relaxation time for the pH gradient is longer: 1-3 min for photocurrent *vs*. ca. 40 min for pH gradient. Total system relaxation and return to dark characteristics is *ca*. 40 min (**Figure 3e**) for the TiO_2 surface used.

The relaxation time depends on morphology and characteristics of the used semiconductor surface. All above mentioned SIET measurements were performed at 100 μm above the surface. To measure variation of the pH as a function of the distance from irradiated TiO_2 surface, the probe microelectrode was moved from 2000 μm to 0 μm distance in Z direction. Interestingly, a linear gradient of the pH was observed in the 0-350 μm range. In the distance from 350 to *appr*. 1000 μm above the TiO_2 surface the pH changes have shown non-linear behavior which can be connected with diffusion of H^+. The pH value above 1250 μm levelled off. In **Figure 3f** the pH is plotted going from 0 μm to 1000 μm Z distance. Thus, *in situ* SIET results prove, that we can effectively modulate the H^+ activity over the surface. Still there remains important questions about separation of the processes of photogeneration of H^+ and OH^- ions laterally over the TiO_2 surface.

We localized the illumination spot and defocused (decreased the intensity of irradiation from 5 mW/cm^2 to 1 mW/cm^2), optical images of the surface with an illumination spot are shown in **Figure 3g** and **Figure 3h**. The SIET map of pH activity is shown in **Figure 3i**, when we decrease the intensity of illumination and locate it at the edge of the measured area. We are able to see on the same surface zone separated H^+ and OH^- activity, which was also assumed looking at **Figure 3b**. Several other conclusions can be suggested based on SIET measurement shown in

Figure 3i: the pH gradient is located in a designed way via the irradiation spot (big advantage in comparison with non-flexible pre-designed electrode pH localization). It is possible to further modify the system to have a pH gradient, (**Figure 1**) and it is worth to discuss with respect to flexible surface process localization. The question is, if we can also locate the electrodes at a certain distance to have further flexibility.

We placed two TiO_2 electrodes electrically connected from the back and shined light on one of them (**Figure 4**). The experiment clearly indicates the distinct advantage of the combined use of photo-anodes and -cathodes for the microscale pH gradient profiles of both H^+ and OH^-. On the irradiated electrode the positive current is detected *vs*. the negative one on the non-irradiated one (**Figure 4c**), however electrodes are located in the same epoxy holder and the same solution. pH maps follow the tendency of the photocurrent: there is acidification on the irradiated surface and alkalinization on the non-irradiated one (**Figure 4d**).

CONCLUSION

Light illumination of a photoconductive surface generates a conducting point that serves as a photo-anode and cathode, where protons and hydroxide ions are produced, leading to an increase and decrease in the pH gradient in an open system. The flexible spatial addressability is a great advantage for open system modulation. The spatial-temporal localization of light over photo-electrodes allows characterization of gradient profiles without any re-fabrication of electrode patterns. A bimodal electrolysis enables the fine-tuning of gradient profiles and enriches the variety of available gradient patterns. Thus, the superposition of bimodal pH gradients offers a practical solution to spatially modulate pH gradient patterns. As a corollary, this procedure also

enriches the variety of available gradient patterns, which can be applied to many different experiments, such as, to artificially reconstruct and apply complicated biological pH gradient patterns to cells in vitro.

In the study, we introduced a novel life inspired light-addressing method to generate microscale pH gradients, proton pumping, at desired locations on a semiconductor substrate. It is always advantageous, if well studied, reliable materials can be applied to obtain new functions. Here TiO_2 is efficient for "inorganic photoproton" cycling. Light irradiation is spatially patterned by the virtual electrodes selected by light. There are photo-anode and cathode sites for H_2O electrolysis. The electrolysis at the pointed locations produces H^+ and OH^-, thus induces pH changes. The pH imaging with *in situ* SIET successfully demonstrated that pH gradients were generated around the light-addressed areas. The characterization of gradient dimensions generated by different irradiation areas and intensity proved the prominent advantage of the light-addressing technique, in particular, spatial flexible localization of photocathode and photoanode. The high degree of freedom in photoanode and photocathode location is promising for tuning of pH gradient profiles. Another advantage of the present method is the combined use of photoanode and photocathode and time controlled illumination. One can imagine a variety of gradient patterns that can be generated, for example, by multipoint surface simultaneous illumination.

EXPERIMENTAL METHODS

Titanium plates (1 mm thickness, 99.6% purity) were chemically polished in HF/HNO_3 concentrated acid mixtures (1:2 in volume) up to a mirror finish followed by rinsing with deionized water and drying in a stream of air. The two-step anodization was carried out in ethylene glycol with addition of 0.75 wt% NH_4F and 2 vol% H_2O. The anodization procedure

consisted of a potential ramp from 0 to 40 V (sweep rate - 200 mV s^{-1}) followed by holding the potential constant for 1 h. The samples prepared during the first step of anodization were then ultrasonically treated in deionized water to strip off the formed TiO_2 layer and expose the underneath titanium substrate. Afterwards the titanium plate was subjected to the second anodization in the same electrolyte under the same regime to create the TiO_2 film with more ordered structure of vertically aligned nanopores (appr. 60 nm in diameter). Then the resultant film was rinsed with ethanol, kept in ethanol for several hours and dried in a stream of air.

As-prepared titania nanotubular film is amorphous. To induce its crystallization, annealing was carried out at 450^{o}C for 3 h in air at a heating rate of 5 ^{o}C min^{-1}. The annealed samples were then used for the SVET/SIET measurements.

SVET/SIET measurements were performed on samples glued to an epoxy support. A beeswax was utilized to insulate each sample leaving a few mm^2 window exposed to the testing solution, 0.05 M Na_2SO_4. The measurements were made with a commercial system (Applicable Electronics Inc. (USA)) and the ASET software from ScienceWares (USA). The vibrating microelectrode for SVET was an insulated Pt–Ir wire with a Pt black deposited on a spherical tip of 20 μm diameter. The probe was located 100 μm above the surface and vibrated with frequencies of 112 and 67 Hz in the directions, respectively, normal and parallel to the surface with 10 μm amplitude. The time for each SVET map (40x40 points) was about 15 min.

For SIET measurements, H^+-selective microelectrodes were prepared from single-barrelled borosilicate glass capillaries with an outer diameter of 1.5 mm. The P-97 Flaming/Brown Micropipette Puller, (Sutter Instruments Company) was used to shape the cone tip. The diameter of the apex of the tip was 2 μm. The capillaries were then silanized by injecting 200 μl of N,N-dimethyltrimethylsilylamine in a glass preparation chamber at 200 ºC. The membrane for H^+-

selective microelectrodes was composed of 6 wt.% 4-nonadecylpyridine, 93 wt.% 2-nitrophenyloctyl ether and 1 wt.% potassium tetra- kis(4-chlorophenyl)borate. The inner reference solution contained a buffer made of 0.01 M KH_2PO_4 in 0.1 M KCl. The liquid membranes were introduced in the glass tip using an optical microscope with two 3D micromanipulators. The column length of proton sensitive probe was about 25–30 μm. A silver chlorinated wire was inserted into the internal solution as the inner reference electrode. The ion-selective microelectrodes were placed 100 μm above the monitored surface on a 30 x 30 grid (900 data points). The time of acquisition for each SIET data point was 2 s, resulting in a total scan time of about 35 min which also includes the time for the electrode to move from point to point. In some cases the probe was placed in a fixed position, monitoring the pH or SVET response over time. A homemade Ag/AgCl/0.1 M KCl, 0.01 M KH_2PO_4 electrode was used as an external reference electrode. The microelectrodes were mounted on the SVET/SIET system to control the position and program the measurements. A preamplifier of 10^{15} Ω input impedance was used to measure the potential. A move-wait-measure scheme was employed for mapping above the surface.

Photoelectrochemical measurements were performed on Autolab PGSTAT 302N potentiostat in a three-electrode quartz cell equipped with a platinum counter-electrode and a saturated calomel reference electrode (SCE).

Local illumination of the TiO_2 film surface was performed using a setup equipped with a high-intensity UV LED (365 nm; 3 W) supplied by a current stabilizer and a UV light beam focusing system involving several quartz lenses.

AUTHOR INFORMATION

Corresponding Author

*skorb@fas.harvard.edu

ACKNOWLEDGMENT

We acknowledge funding from SMARCOAT project. This project has received funding from the European Union's Horizon 2020 research and innovation programme under the Marie Skłodowska-Curie grant agreement No 645662. J.T. thanks FCT for the research grant IF/00347/2013.

REFERENCES

1. Grzybowski BA, Huck WTS (2016) The nanotechnology of life-inspired systems. *Nature Nanotechnol* 11(7):584-591.
2. Chen JW, Wezenberg SJ, Feringa BL (2016) Intramolecular transport of small-molecule cargo in a nanoscale device operated by light. *Chem Comm* 52(41):6765-6768.
3. Kudernac T*, et al.* (2011) Electrically driven directional motion of a four-wheeled molecule on a metal surface. *Nature* 479(7372):208-211.
4. Eelkema R*, et al.* (2006) Nanomotor rotates microscale objects. *Nature* 440(7081):163-163.
5. Wong ASY, Postma SGJ, Vialshin IN, Semenov SN, Huck WTS (2015) Influence of Molecular Structure on the Properties of Out-of-Equilibrium Oscillating Enzymatic Reaction Networks. *J Am Chem Soc* 137(38):12415-12420.
6. Hermans TM, Stewart PS, Grzybowski BA (2015) pH Oscillator Stretched in Space but Frozen in Time. *J Phys Chem Lett* 6(5):760-766.
7. Semenov SN*, et al.* (2016) Autocatalytic, bistable, oscillatory networks of biologically relevant organic reactions. *Nature* 537(7622):656-660.
8. Ichimura K (2002) Nonlinear organic reactions to proliferate acidic and basic molecules and their applications. *Chem Rec* 2(1):46-55.
9. Whitesides GM (2015) Bioinspiration: something for everyone. *Interface Focus* 5(4): 1-10.
10. Semenov SN*, et al.* (2015) Rational design of functional and tunable oscillating enzymatic networks. *Nature Chem* 7(2):160-165.
11. Kato M, Zhang JZ, Paul N, Reisner E (2014) Protein film photoelectrochemistry of the water oxidation enzyme photosystem II. *Chem Soc Rev* 43(18):6485-6497.
12. Rivera-Chavez F, Baumler AJ (2015) The Pyromaniac Inside You: Salmonella Metabolism in the Host Gut. *Ann Rev Microbiol,* 69:31-48.
13. Koumura N, Zijlstra RWJ, van Delden RA, Harada N, Feringa BL (1999) Light-driven monodirectional molecular rotor. *Nature* 401(6749):152-155.

14. Skorb EV, Möhwald H, Andreeva DV (2017) How can one controllably use of natural ΔpH in polyelectrolyte multilayers? *Adv Mater Interfaces* 4:1600282.
15. Ulasevich SA*, et al.* (2016) Light-Induced Water Splitting Causes High-Amplitude Oscillation of pH-Sensitive Layer-by-Layer Assemblies on TiO_2. *Angew Chem Int Ed* 55(42):13001-13004.
16. Ulasevich SA*, et al.* (2016) Switching the Stiffness of Polyelectrolyte Assembly by Light to Control Behavior of Supported Cells. *Macromol Biosci* 16(10):1422-1431.
17. Andreeva DV, Melnyk I, Baidukova O, Skorb EV (2016) Local pH Gradient Initiated with Light on TiO_2 for Light-Triggered Polyhistidine-Tagged Proteins Modulation. *ChemElectroChem* 3:1306-1310.
18. Shchukin DG, Sviridov DV (2006) Photocatalytic processes in spatially confined micro- and nanoreactors. *J Photochem Photobiol C-Photochem Rev* 7(1):23-39.
19. May MM, Lewerenz HJ, Lackner D, Dimroth F, Hannappel T (2015) Efficient direct solar-to-hydrogen conversion by in situ interface transformation of a tandem structure. *Nature Comm* 6:1-7.
20. Chen HH, Nanayakkara CE, Grassian VH (2012) Titanium Dioxide Photocatalysis in Atmospheric Chemistry. *Chem Rev* 112(11):5919-5948.
21. Skorb EV*, et al.* (2008) Antibacterial activity of thin-film photocatalysts based on metal-modified TiO_2 and TiO_2:In_2O_3 nanocomposite. *Appl. Cat. B-Environmental* 84(1-2):94-99.
22. Schneider J*, et al.* (2014) Understanding TiO_2 Photocatalysis: Mechanisms and Materials. *Chem Rev* 114(19):9919-9986.
23. Byk TV*, et al.* (2008) Photochemical selective deposition of nickel using a TiO_2-Pd^{2+} layer. *J Photochem Photobiol A-Chem* 193(1):56-64.
24. Skorb EV*, et al.* (2010) Titania-assisted electron-beam and synchrotron lithography. *Nanotechnology* 21(31): 1-5.
25. Skorb EV, Sokolov VG, Gaevskaya TV, Sviridov DV (2009) Photocatalytic lithography with image inversion. *Theor Experimental Chem* 45(1):40-43.
26. Green JR, Costa AB, Grzybowski BA, Szleifer I (2013) Relationship between dynamical entropy and energy dissipation far from thermodynamic equilibrium. *Proc Natl Acad Sci USA* 110(41):16339-16343.
27. Emond M*, et al.* (2012) Energy Propagation Through a Protometabolism Leading to the Local Emergence of Singular Stationary Concentration Profiles. *Chem-A European J* 18(45):14375-14383.
28. Yoshida R, Ueki T (2014) Evolution of self-oscillating polymer gels as autonomous polymer systems. *NPG Asia Materials* 6:1-14.
29. Skorb EV, Möhwald H (2013) 25th Anniversary Article: Dynamic Interfaces for Responsive Encapsulation Systems. *Advanced Materials* 25(36):5029-5042.
30. Jha PK, Kuzovkov V, Grzybowski BA, de la Cruz MO (2012) Dynamic self-assembly of photo-switchable nanoparticles. *Soft Matter* 8(1):227-234.
31. Wei YK, Su JZ, Wan XK, Guo LJ, Vayssieres L (2016) Spontaneous photoelectric field-enhancement effect prompts the low cost hierarchical growth of highly ordered heteronanostructures for solar water splitting. *Nano Research* 9(6):1561-1569.
32. Kopf J*, et al.* (2016) Ultrasonically Produced Porous Sponge Layer on Titanium to Guide Cell Behavior. *Adv Eng Mater* 18(4):476-483.

33. Nakamura R, Nakato Y (2004) Primary intermediates of oxygen photoevolution reaction on TiO_2 (rutile) particles, revealed by in situ FTIR absorption and photoluminescence measurements. *J Am Chem Soc* 126(4):1290-1298.
34. Nakamura R, Imanishi A, Murakoshi K, Nakato Y (2003) In situ FTIR studies of primary intermediates of photocatalytic reactions on nanocrystalline TiO_2 films in contact with aqueous solutions. *J Am Chem Soc* 125(24):7443-7450.
35. Xiang QJ, Yu JG, Jaroniec M (2011) Enhanced photocatalytic H-2-production activity of graphene-modified titania nanosheets. *Nanoscale* 3(9):3670-3678.
36. Suzurikawa J, Nakao M, Kanzaki R, Takahashi H (2010) Microscale pH gradient generation by electrolysis on a light-addressable planar electrode. *Sensors and Actuators B-Chem* 149(1):205-211.
37. Fiedler S*, et al.* (1995) Diffusional Electrotitration - Generation of Ph Gradients over Arrays of Ultramicroelectrodes Detected by Fluorescence. *Anal Chem* 67(5):820-828.

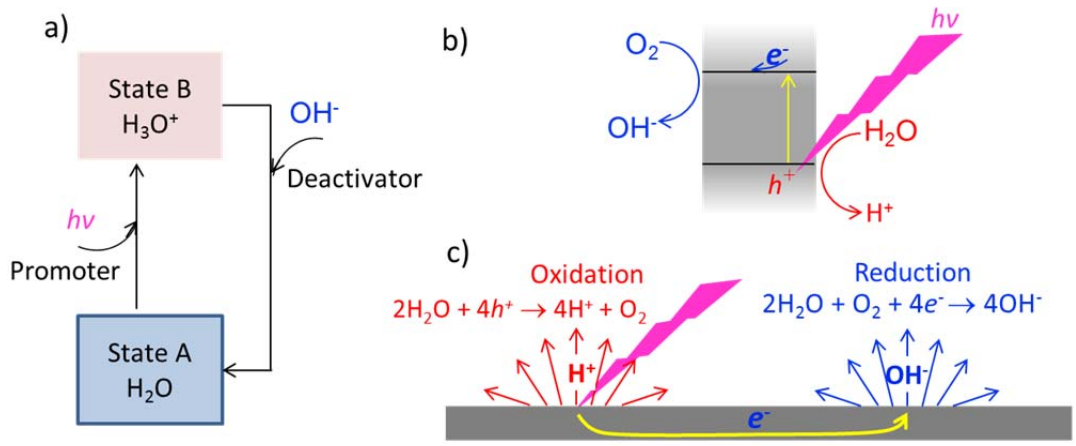

Figure 1. Suggested system for life inspired proton pumping on a semiconductor. (a) Simplest chemical networking in focus. (b) Light induces charge separation in a nanostructured semiconductor and a red/ox reaction with production of H^+ and OH^-. (c) Separation of the redox processes on semiconductor surface for the development of localized chemical networking, where the localization is determined by the position of the irradiation spot and is flexible.

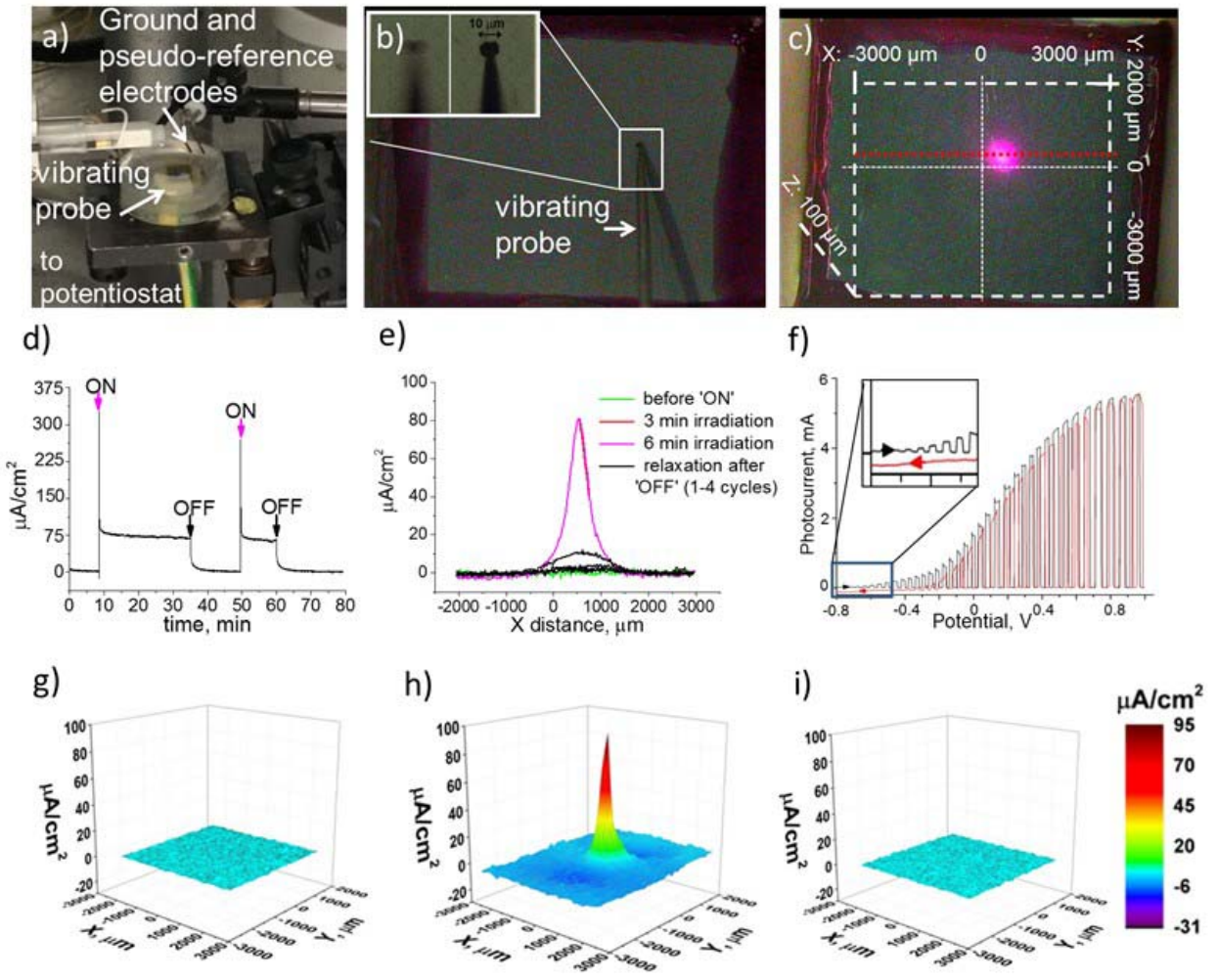

Figure 2. SVET measurements of ionic current density in electrolyte. Current density can be attributed to photocurrent. (a) Set-up of *in situ* scanning vibrating electrode technique (SVET) to analyze local current densities in electrolyte associated with photocurrents generated on a TiO_2 layer; (b) sample with vibrating probe before irradiation; (c) sample with the position of maps (white lines), line measurements (red line) and place of irradiation (bright spot in center of sample). (d) Ionic current density in electrolyte above the irradiated spot on a titania layer under switching on and switching off the light. (e) SVET current density measured in lines every 3 minutes before, during and after irradiation. (f) Current-potential curve recorded under chopped illumination for TiO_2. (g-i) SVET maps (g) before irradiation; (h) during local irradiation; and (i) after irradiation (after 5 min of relaxation). The measurements were performed in 0.05M Na_2SO_4.

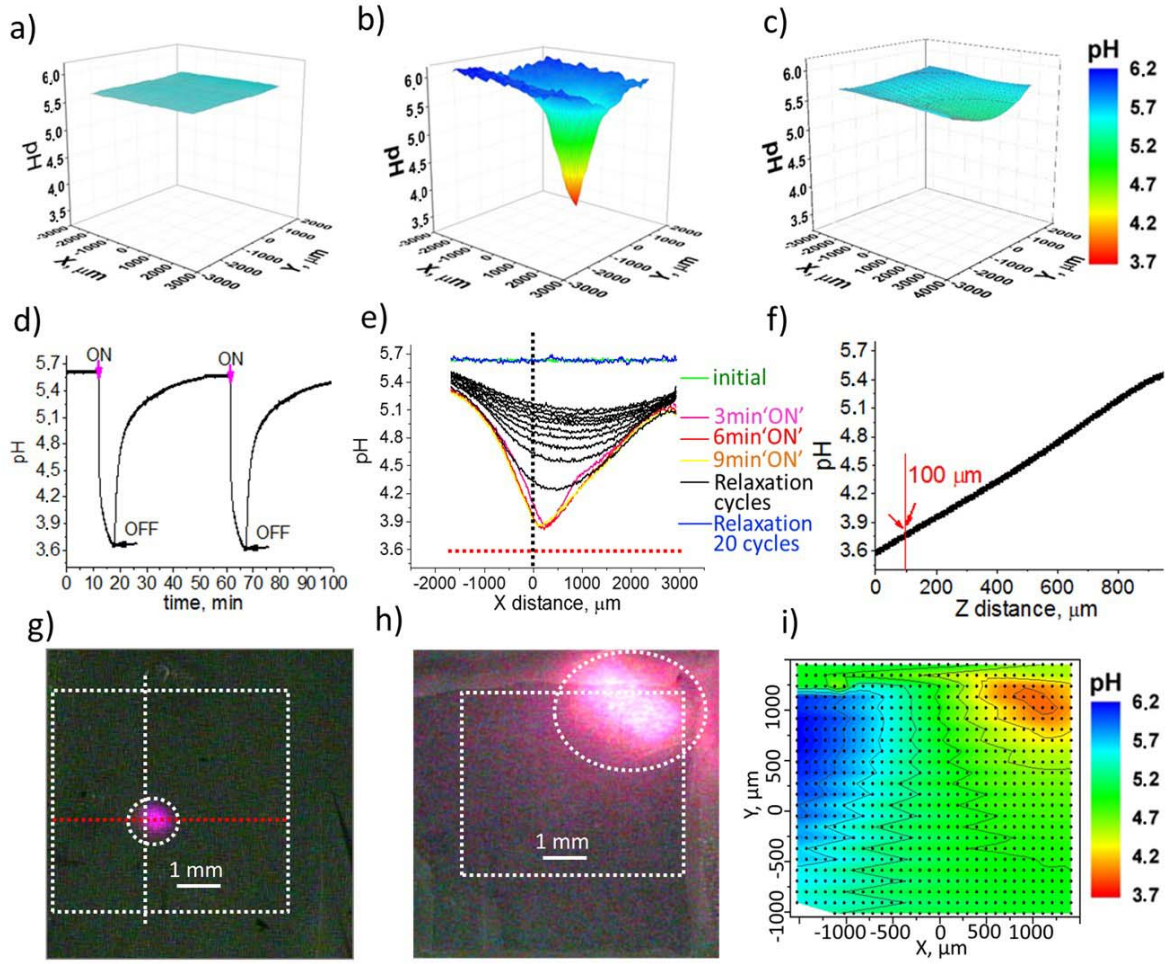

Figure 3. Light induced flexible pH gradient and proton pumping. Maps obtained by the in situ scanning ion selective electrode technique (SIET) to analyze local pH gradients generated on nanostructured TiO_2: (a) before irradiation; (b) during local irradiation; and (c) after irradiation (20 min of relaxation). (d) pH measurement inside an irradiation spot (shown in (g)), single spot time evolution measurements, on a titania layer under switching on and switching off the light. (e) local pH measurements in a line (shown in (g) in red) before, during and after irradiation (maximum coincides with the position of the irradiating spot, the time of measurement of each line was 3 minutes). (f) pH in Z-direction during illumination inside irradiated spot. (g) Optical image of the surface and location of the focused irradiation spot on TiO_2 described above (a-e) mapped in (a-c). (h) Optical image with defocused light to show the flexibility of the method to change intensity of illumination and its location and effect on the pH gradient of the surface with corresponding (i) pH map with color pointed acidic and basic pH areas.

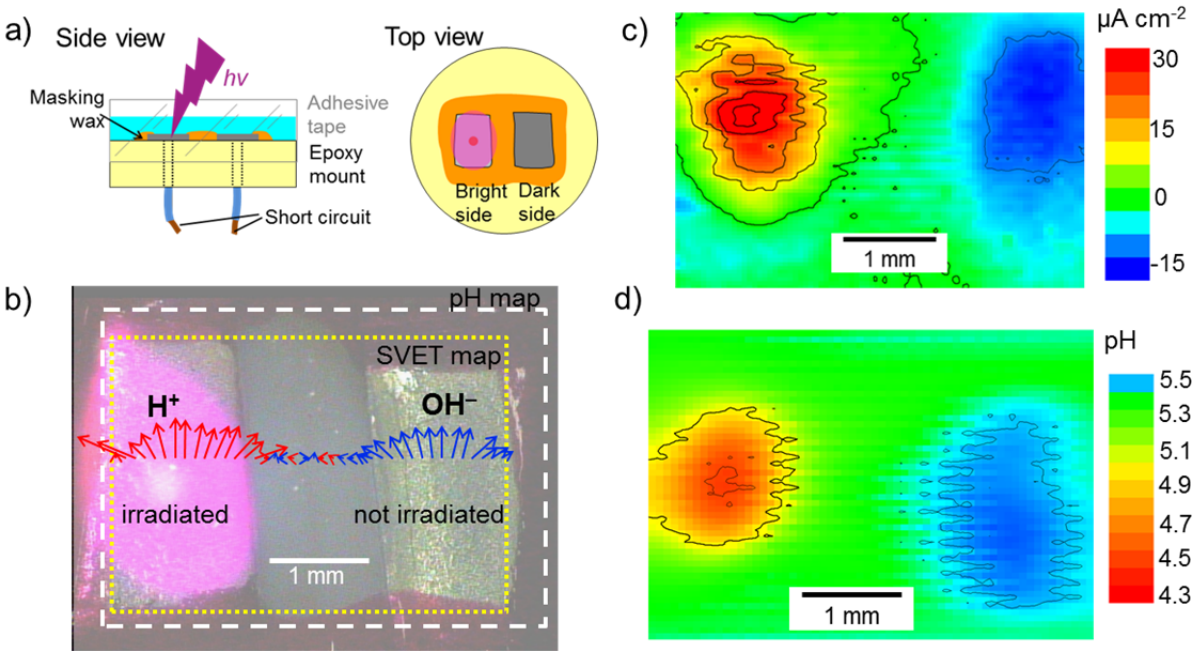

Figure 4. Prospects of chemical networking in open system. (a) Schematics of the electrochemical cell used for studying local changes in the electrolyte created by the spatial separation of light stimulated reactions on TiO_2. (b) Image of the cell surface with the two TiO_2 electrodes, one irradiated, with primary reaction with photohole, production of proton and local acidification and another non irradiated with local production of hydroxide ions. The arrows are 2D vectors of the current density measured by SVET associated to the oxidation (red) and reduction (blue) reactions. Also depicted are the positions of SVET and pH maps. (c) SVET map of the current density in solution crossing a plane parallel to the surface 100 µm above it with positive (anodic) currents in the irradiated area and negative (cathodic) currents in the non irradiated areas. (d) SIET pH map showing local acidification in the irradiated spot and alkalization in the non irradiated area.